

The production and characterization of bonded, hot-pressed and die-upset HDDR magnets

P. J. McGuinness, C. Short, A. F. Wilson* and I. R. Harris

School of Metallurgy and Materials, University of Birmingham, Birmingham B15 2TT (UK)

(Received November 11, 1991)

Abstract

The recently developed hydrogenation, disproportionation, desorption and recombination (HDDR) process has now been extended to the production of hot-pressed isotropic magnets. These magnets have been produced from cast alloy with a composition $\text{Nd}_{16}\text{Fe}_{76}\text{B}_8$ and exhibit intrinsic coercivities of about 1200 kA m^{-1} , remanences of around 690 mT and BH (max) values of approximately 90 kJ m^{-3} . Subsequent die upsetting indicates that increased remanences can be obtained by using a suitable height reduction ratio.

Careful studies of the microstructures of the isotropic hot-pressed magnets reveal that they are similar to the HDDR material in its powder form, *i.e.* they consist of $\text{Nd}_2\text{Fe}_{14}\text{B}$ grains predominantly in the range $0.1 \leq x \leq 1.0 \mu\text{m}$ with a very small number of grains in the range $10 \leq x \leq 35 \mu\text{m}$. These larger grains exhibit a very regular morphology and appear to be the result of a very rapid growth of some of the smaller submicron grains. The starting composition of the cast material ensures that the magnets have about 12% neodymium rich intergranular material and this low melting point constituent has been found to be of great assistance in the densification process. However, scanning and transmission electron microscopy studies show that the neodymium rich material is very coarsely distributed throughout the hot-pressed magnet and little evidence can be found for its presence between the grains of $\text{Nd}_2\text{Fe}_{14}\text{B}$.

The addition of small amounts of zirconium to the basic $\text{Nd}_{16}\text{Fe}_{76}\text{B}_8$ alloy was investigated to determine its effect on coercivity and grain orientation. Highly oriented powder with good coercivity has been produced from material containing 0.1 at.% Zr ($\text{Nd}_{16}\text{Fe}_{76.9}\text{B}_8\text{Zr}_{0.1}$). Larger zirconium additions resulted in significant losses in coercivity. Bonded magnets with a remanence of about 1050 mT , an intrinsic coercivity of 740 kA m^{-1} and an energy product of about 150 kJ m^{-3} have been produced from the anisotropic HDDR powder.

1. Introduction

Hydrogen is now well established as an integral part of the production of NdFeB-type permanent magnets. The hydrogen decrepitation (HD)

*Teaching Company Associate at Philips Components Ltd., Crossens, Southport, Merseyside PR9 8PZ, UK.

process (see *e.g.* ref. 1), whereby hydrogen is used to break up and embrittle the ingot prior to jet milling, is used by magnet manufacturers around the world as an alternative to conventional hammering and crushing techniques.

Developments in Japan [2] and Europe [3] have shown that hydrogen processing at elevated temperatures can be used to produce highly coercive isotropic powder directly from the cast ingot. This procedure, now known as the hydrogenation, disproportionation, desorption and recombination (HDDR) process, results in powder which can be mixed with epoxy to make isotropic bonded magnets. The process requires that the starting material, typically in the composition range $\text{Nd}_{12}\text{Fe}_{82}\text{B}_6$ to $\text{Nd}_{16}\text{Fe}_{76}\text{B}_8$, be disproportionated by exposure to hydrogen at high temperatures. The material is subsequently recombined under vacuum at temperatures in the region 750–830 °C. The disproportionation of the $\text{Nd}_2\text{Fe}_{14}\text{B}$ (matrix) phase takes place at 720 °C using a pressure of around 1 bar hydrogen. The role of this reaction in producing coercive material was first established by McGuinness *et al.* [4] using X-ray diffraction and magnetic studies which revealed that the material consisted primarily of finely divided iron, ferroboron (Fe_2B) and neodymium hydride. On desorbing the hydrogen from the neodymium hydride under vacuum at elevated temperature, the iron, Fe_2B and neodymium mixture becomes thermodynamically unstable and reverts to the more stable $\text{Nd}_2\text{Fe}_{14}\text{B}$ phase. On re-formation the $\text{Nd}_2\text{Fe}_{14}\text{B}$ forms very fine crystals and thus the HDDR process converts the relatively coarse-grained cast ingot into a material with an ultrafine (below 1 μm) structure.

The HDDR powder appears to be a very suitable material for subsequent bonding and hot pressing. The roughly spherical nature of the processed powder would lend itself to injection-moulding techniques where a high degree of flowability is required. The possibility of producing very smooth and spherical powder has recently been investigated in the USA [5], where spherical HDDR powder has been produced not from the cast alloy but from a gas-atomized powder. This powder was found to exhibit coercivities of about 11 kOe, although significant variation was found throughout the processed batch unless the HDDR process was repeated a second time. This second HDDR cycle also resulted in a further 15%–80% increase in the intrinsic coercivity (depending on the position of the material in the furnace and the starting composition of the alloy).

In this paper we report our studies on varying the processing parameters for powder production and the necessary conditions for successful hot pressing. We have looked at the potential for producing high energy product, fully dense samples by combining a die-upsetting stage with the hot pressing. Following on from reports by Takeshita and Nakayama [6] that the addition of elements such as zirconium, hafnium or gallium induces a preferred orientation of growth during the recombination stage, a range of alloys containing varying amounts of zirconium have been investigated. The resulting anisotropic powder has been bonded to produce anisotropic bonded magnets with a record $BH(\text{max})$ for this type of material.

2. Powder processing

Ingot pieces of an alloy of composition $\text{Nd}_{16}\text{Fe}_{76}\text{B}_8$ supplied by Rare Earth Products plc were placed in the chamber of a combined hydrogenation–vacuum–annealing system. The chamber was evacuated to less than 10^{-1} mbar prior to being filled with pure hydrogen to a pressure of about 0.5 bar from an LaNi_5 hydride store. After completion of the room temperature absorption stage (in effect the HD process) the sample was heated in a hydrogen atmosphere at $10\text{ }^\circ\text{C min}^{-1}$ to $740\text{--}820\text{ }^\circ\text{C}$ while maintaining a pressure of about 0.5 bar. A second, smaller absorption was observed at about $720\text{ }^\circ\text{C}$ and this corresponds to the point where the $\text{Nd}_2\text{Fe}_{14}\text{B}$ hydride disproportionates into the more thermodynamically stable mixture of iron, Fe_2B and neodymium hydride. The sample was held at this temperature under hydrogen for 2 h to ensure completion of the disproportionation stage before the hydride was desorbed by evacuation using a conventional rotary pump. This resulted in the conversion of the neodymium hydride to neodymium metal and the mixture of neodymium, Fe_2B and iron then recombined to form $\text{Nd}_2\text{Fe}_{14}\text{B}$. After 1 h under vacuum the constitution of the material returned to its original state consisting of the majority $\text{Nd}_2\text{Fe}_{14}\text{B}$ phase with small amounts of neodymium-rich material and a little NdFe_4B_4 (the latter being unaffected by the disproportionation process [4]). The above changes were accompanied by a significant modification of the microstructure, with the $\text{Nd}_2\text{Fe}_{14}\text{B}$ matrix phase now mainly in the form of approximately $0.3\text{ }\mu\text{m}$ grains and the individual particles (around $250\text{ }\mu\text{m}$ in diameter) exhibiting a high intrinsic coercivity. It has been noted [2] that the optimum grain size for the HDDR material is very close to that of the single-domain size for $\text{Nd}_2\text{Fe}_{14}\text{B}$.

Samples of HDDR material processed over the range of temperatures were bonded using a conventional “Metset” resin so as to allow measurement of the intrinsic coercivity of the powder with a conventional permeameter. The results of this investigation are shown in Fig. 1. The relatively sharp peak in the variations in coercivity *vs.* temperature indicates the importance

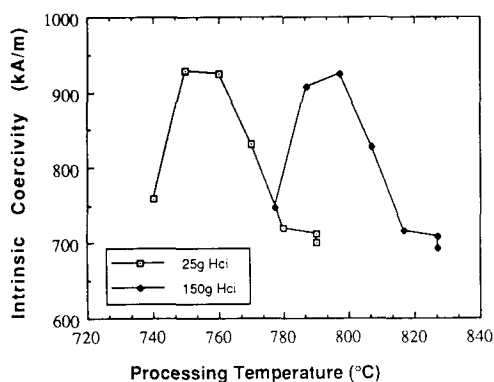


Fig. 1. Intrinsic coercivity of HDDR powder *vs.* processing temperature.

of temperature as a process variable. Earlier investigations [3, 7] have indicated that the reduced coercivity resulting from processing at too low a temperature is because of incomplete homogenization of the initial alloy and incomplete recombination of the material, with the result that magnetically soft iron is contained within the sample. Because iron is soft magnetically, it is detrimental to the permanent magnetic properties. This work [3, 7, 8] also showed that the lower coercivity observed on the high temperature side of the curve can be attributed to the rapid growth of a large number of the previously submicron grains. These grains can be observed growing with a very regular morphology and to a considerable size, *i.e.* greater than 100 μm . In an investigation carried out by Zhang *et al.* [9] these grains were often observed to be growing with a rectangular morphology with the *a* and *c* axes running parallel to the sides of the rectangular grain.

Initially, magnetic samples were produced in batches of 25 g and the maximum coercivity was found for a processing temperature of 755 °C. In an attempt to produce larger quantities of material the batch size was increased to 150 g. Processing this sample at 755 °C resulted in a very poor coercivity being obtained and further investigation revealed that the optimum processing temperature for this larger quantity of material was some 30 °C higher (Fig. 1). This can be attributed to the additional quantity of desorbed hydrogen in this case and the fixed pumping rate of the vacuum system employed. Thus to remove all the hydrogen for the same time a higher temperature is required. This change in conditions for different quantities of alloy was also commented on by Takeshita and Nakayama [6], who did not present results but stated "The evacuation time for the recrystallization step of course depends on temperature, amount of powder, and the pumping capacity of the system to be used". This effect is important since it indicates that there may be some problems to overcome if the process is to be "scaled up significantly" and the quantity of material and the performance of the pumping system would have to be monitored carefully.

3. Fabrication of hot-pressed magnets

The isotropic HDDR powder produced from the $\text{Nd}_{16}\text{Fe}_{76}\text{B}_8$ alloy which exhibited an intrinsic coercivity of about 970 kA m^{-1} in the bonded state was precompacted into 8 g cylinders of 12.5 mm diameter. The cylinders were sprayed with a lubricant and then placed on the carousel of the hot-pressing machine. Each sample was then loaded automatically into the press and preheated to 650–850 °C for 20 s prior to pressing with 2.5 t cm^{-2} at the same temperature for a further 20 s. The now fully dense or nearly fully dense samples were ejected from the bottom of the die and allowed to cool to room temperature in a stream of argon gas. Preliminary results on these magnets have been reported elsewhere [10].

The preheating and pressing temperatures were varied between 650 and 850 °C (with preheating temperature equal to pressing temperature). Figures

2–5 show respectively the variations in density, remanence, intrinsic coercivity and $BH(\max)$ with temperature. The density increases linearly with increasing temperature from 650 to 730 °C. From 730 to 850 °C no further increase is observed and the density of the hot-pressed samples reached 7.44–7.46 g cm⁻³, *i.e.* close to the theoretical maximum for this particular alloy. The change in density is matched by the change in remanence. This is the behaviour that would be expected from such a system and results in a maximum remanence of 715 mT and an average value of 690 mT. No further increase in remanence is seen at pressing temperatures greater than 730 °C. The coercivity exhibits a somewhat less predictable behaviour although general trends can be observed. It increases quite sharply from the value of about 970 kA m⁻¹ obtained when the material is in the form of bonded HDDR powder to values of about 1250 kA m⁻¹ when pressed at 750 °C. At higher processing temperatures a rapid fall-off in the intrinsic coercivity is observed, which is probably due to rapid grain growth at these temperatures.

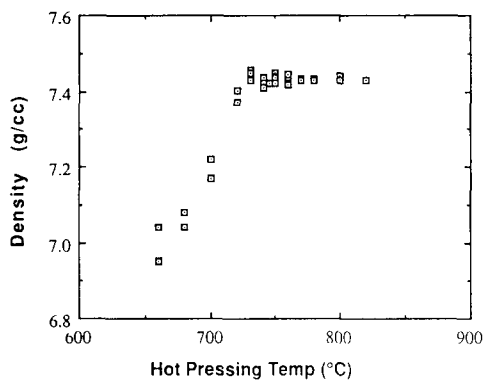


Fig. 2. Density of hot-pressed magnet *vs.* hot-pressing temperature.

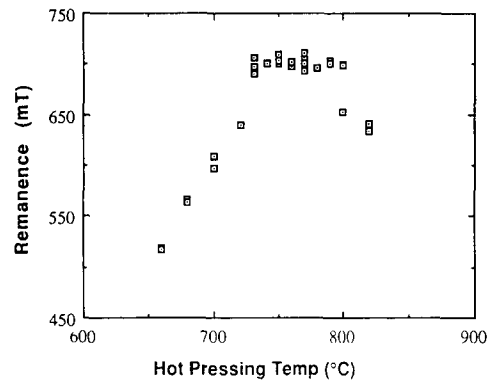


Fig. 3. Remanence of hot-pressed magnet *vs.* hot-pressing temperature.

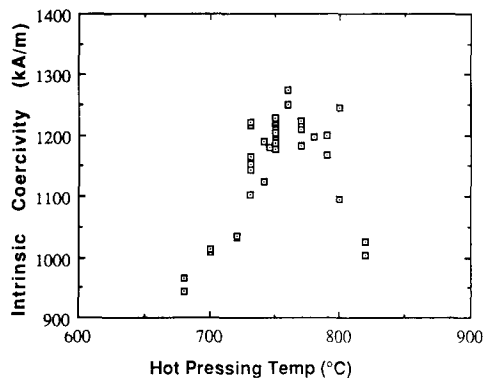


Fig. 4. Intrinsic coercivity of hot-pressed magnet *vs.* hot-pressing temperature.

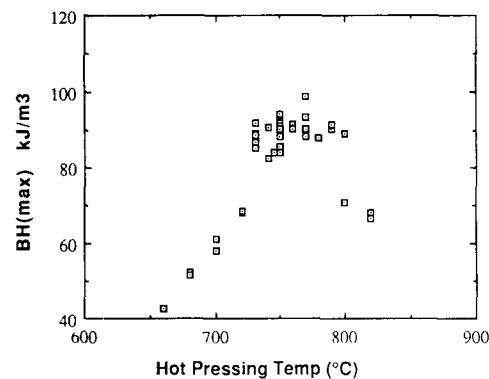


Fig. 5. Maximum energy product of hot-pressed magnet *vs.* hot-pressing temperature.

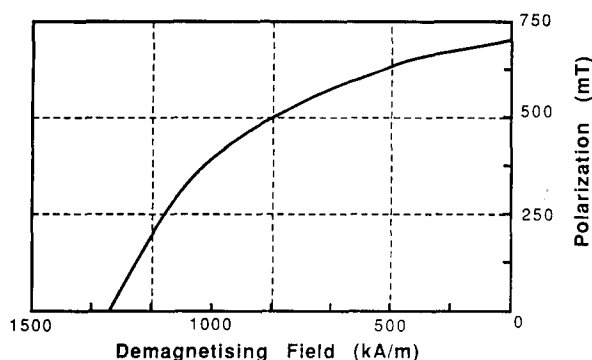


Fig. 6. Second-quadrant demagnetization curve of HDDR hot-pressed magnet.

It is interesting to note that under optimum processing conditions a substantial increase in coercivity over that determined in the bonded powder sample is obtained.

The graph of maximum energy product follows a similar trend to that of the remanence *vs.* temperature curve, with a maximum of 90 kJ m^{-3} obtained for preheating and pressing the material at 740°C . A typical second-quadrant demagnetization curve for the magnets is shown in Fig. 6.

The large quantity of excess neodymium in the $\text{Nd}_{16}\text{Fe}_{76}\text{B}_8$ alloy appears to be necessary to facilitate the hot-pressing operation. Significant coercivities can be achieved with near-stoichiometric $\text{Nd}_{2.1}\text{Fe}_{14}\text{B}$ materials [9], but compacts produced from these samples cannot be fully densified under normal hot-pressing conditions [11].

4. Die upsetting of hot-pressed HDDR magnets

A number of the hot-pressed fully dense samples were reduced in diameter using a computer-controlled spark-cutting machine so that they could be repositioned in the original hot-pressing cavity and pressed again under the same conditions as described above, causing each sample to be die upset forged. The degree to which each of these samples was die upset (expressed as the ratio h_0/h , where h_0 is the original height and h is the final height) depended on the sample diameter. In this experiment die-upset samples were produced in the range $h_0/h = 1$ (no die upsetting) to $h_0/h = 3$ (a reduction to 33% of the original height). The samples were easy to process and none of the magnets exhibited cracks to any significant degree. The die-upset-forged samples showed an increase in remanence comparable with that observed by Tokunaga *et al.* [12], who carried out die-upsetting experiments on MagneQuench (MQ)-type materials. A comparison of the data points obtained with those of Tokunaga *et al.* [12] (see Figs. 7(a) and 7(b)) indicates that fully anisotropic HDDR magnets could be produced by using an upsetting ratio $h_0/h \approx 5$ (a reduction to 20% of the original height). Again it is interesting

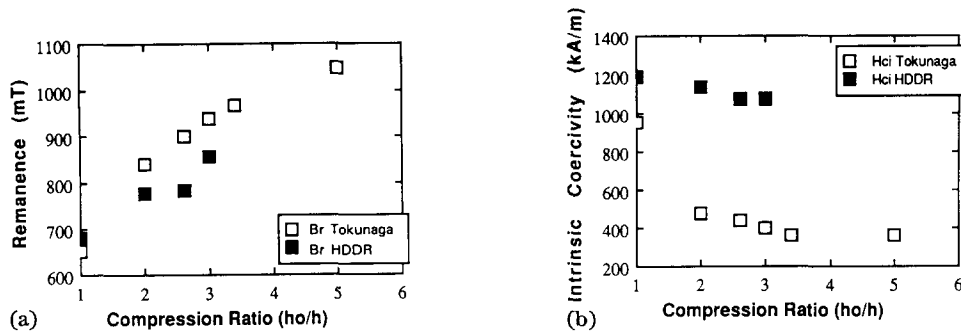


Fig. 7. Comparison of (a) remanences and (b) coercivities obtained from die-upset HDDR magnet with those obtained for MQ-type material.

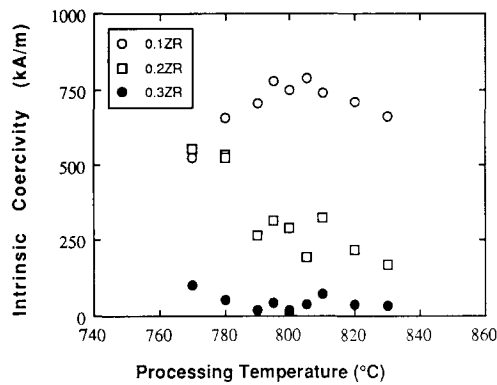


Fig. 8. Intrinsic coercivity of 0.1Zr, 0.2Zr and 0.3Zr materials vs. processing temperature.

to note that the large decrease in coercivity observed by Tokunaga *et al.* after die upsetting the MQ-type materials is not observed in the case of die upsetting the HDDR materials (Fig. 7(b)).

5. Additions of zirconium to the $\text{Nd}_{16}\text{Fe}_{76}\text{B}_8$ alloy

The work of Takeshita and Nakayama [6] covered additions of $M \equiv \text{Al}, \text{Ga}, \text{In}, \text{Si}, \text{Ge}, \text{Sn}, \text{Ti}, \text{Zr}, \text{Hf}, \text{V}, \text{Nb}, \text{Ta}, \text{Cu}, \text{Zn}, \text{Sb}$ and Bi to the near-stoichiometric composition $\text{Nd}_{12.5}\text{Fe}_{70-x}\text{Co}_{11.5}\text{B}_6\text{M}_x$ and indicated that $M \equiv \text{Zr}, \text{Hf}$ and Ga were promising additions for inducing anisotropic HDDR materials. We have carried out a detailed investigation of the effects of zirconium additions to the $\text{Nd}_{16}\text{Fe}_{76-x}\text{B}_8\text{Zr}_x$ alloy, which is similar to the ternary composition used for powder sintering and which we have found to be ideal for hot pressing. The alloys selected for investigation were $\text{Nd}_{16}\text{Fe}_{75.9}\text{B}_8\text{Zr}_{0.1}$, $\text{Nd}_{16}\text{Fe}_{75.8}\text{B}_8\text{Zr}_{0.2}$ and $\text{Nd}_{16}\text{Fe}_{75.7}\text{B}_8\text{Zr}_{0.3}$. Each sample was investigated by processing HDDR powder in a range of temperatures from 760 to 840 °C using the conventional (2 h under hydrogen, 1 h under vacuum plus cooling) method. Figure 8 shows the observed variations in coercivity with processing

temperature for the 0.1Zr, 0.2Zr and 0.3Zr alloys. The 0.3Zr material exhibits consistently low properties, with all the coercivities being below 120 kA m^{-1} and an average value of 45 kA m^{-1} . In contrast, the 0.1Zr material exhibits behaviour very similar to that of the conventional $\text{Nd}_{16}\text{Fe}_{76}\text{B}_8$ alloy, with the peak in the coercivity of about 800 kA m^{-1} at a processing temperature of $795 \text{ }^\circ\text{C}$, just $10 \text{ }^\circ\text{C}$ higher than that for an equivalent mass of the zirconium-free $\text{Nd}_{16}\text{Fe}_{76}\text{B}_8$ alloy. From the results obtained for the 0.2Zr alloy a clear pattern does not emerge. It is possible that the general slope indicates a peak in the coercivity at lower temperatures, but this could present problems in achieving good properties since at temperatures below $760 \text{ }^\circ\text{C}$ it is not possible to remove all the hydrogen from the material without significantly extending the processing time or altering other experimental parameters such as the pumping rate. It is also possible that a certain degree of inhomogeneity is present in this particular sample and this would not be surprising in a sample with such small additions of zirconium and where the zirconium has been shown to have such a significant effect.

Bonded test samples of HDDR powders from the 0.1Zr and 0.2Zr alloys were produced by mixing the coercive material with conventional "Metset" resin. Two samples were produced from each of the powders: sample 1 was allowed to set without any applied magnetic field whereas, sample 2 was subjected to a magnetic field of about 1.5 T during setting. Each sample was then measured using a permeameter and the approximate degree of alignment was determined using the equation

$$\text{degree of alignment} = \frac{Br_2 - Br_1}{Br_1}$$

where Br_2 is the remanence of the aligned sample and Br_1 is the remanence of the isotropic sample

All the samples produced from the 0.1Zr material had an alignment factor greater than 89%, with an average value of 95%. The 0.2Zr material was found to have slightly poorer alignment characteristics, with a minimum alignment factor of 83% and an average value of 89%. These represent remarkable increases over the (in effect, isotropic) value of 53% obtained for the conventional HDDR $\text{Nd}_{16}\text{Fe}_{76}\text{B}_8$ powder when set in a magnetic field. The poor magnetic properties of 0.3Zr made it impossible to determine an alignment factor for this material.

6. Resin-bonded magnets from $\text{Nd}_{16}\text{Fe}_{75.9}\text{B}_8\text{Zr}_{0.1}$ alloy

In an attempt to achieve maximum properties from the anisotropic HDDR magnetic powder, bonded magnets were produced using high loadings of the magnetic material. Samples were produced from about 25 g of powder with the minimum amount of epoxy resin necessary to produce a robust finished magnet. The optimum mixture of powder (density 7.5 g cm^{-3}) and resin (density 1.15 g cm^{-3}) was found to be 80:20 by volume. The material

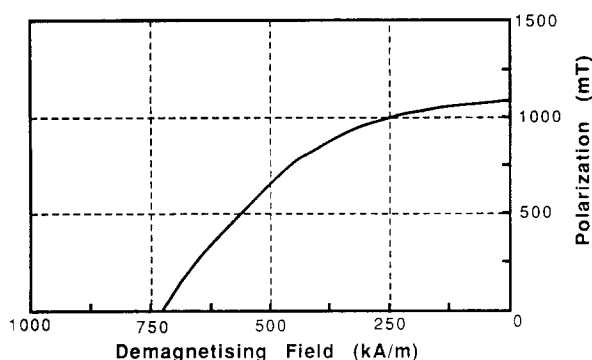


Fig. 9. Second-quadrant demagnetization curve of bonded magnet from 0.1Zr powder.

was pressed in a field of approximately 1.4 T with a pressing force of 10 t acting on a tungsten carbide die 30 mm in diameter. A very small amount (less than 1 wt.%) of die lubricant was used to prevent excess wear on the die. The aligned sample was then ejected from the die and cured in an open furnace for 1 h at 170 °C.

The magnets exhibited very high remanences of around 1050 mT, as would be expected from the use of anisotropic powder, and a coercivity of 700 kA m⁻¹ (slightly less than that achieved under isotropic conditions). A resulting energy product of about 150 kJ m⁻³ was obtained. A typical second-quadrant demagnetization curve is shown in Fig. 9.

7. Microstructural investigations of isotropic and anisotropic HDDR material

The HDDR powder produced from Nd₁₆Fe₇₆B₈ material was observed using a high resolution Hitachi 4000 scanning electron microscope. Figure 10 shows three approximately 200 μm particles of this powder. The material is characteristically equiaxed in shape, which indicates that they are probably the grains of the original cast structure. A very high magnification photograph of the surface of a particle reveals that it is made up of small domed regions (Fig. 11). These domes are consistent with the growth of approximately of 0.3 μm grains of Nd₂Fe₁₄B within the large powder particle.

The microstructural changes which take place during the HDDR process are shown clearly in Fig. 12. Figure 12(a) shows the original cast microstructure typical of alloys with the Nd₁₆Fe₇₆B₈ composition, while Fig. 12(b) shows the material after processing: the original grain boundaries are still visible, but what was once a single grain of Nd₂Fe₁₄B is now a region of many submicron Nd₂Fe₁₄B grains. As a result of the hot-pressing operation a fully dense body is formed, and a polished sample (Fig. 13) viewed in the scanning electron microscope shows that the magnet appears to consist of large (approximately 250 μm) areas of Nd₂Fe₁₄B with surrounding neodymium-rich material. The fracture surface (Fig. 14) of one of the magnets indicates,

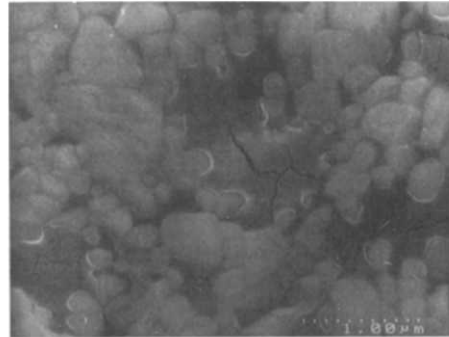
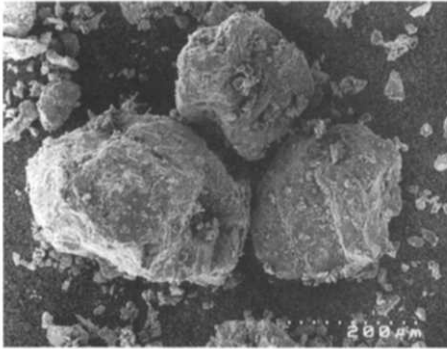
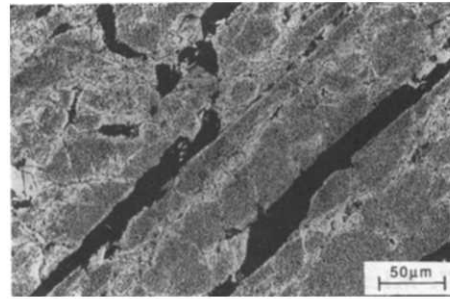
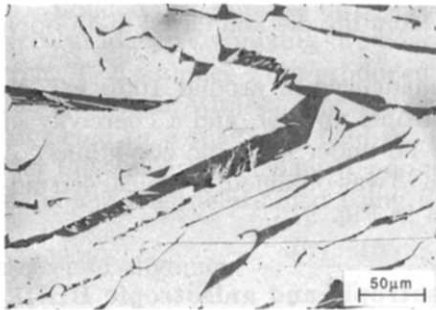


Fig. 10. Scanning electron micrograph of HDDR powder particles.

Fig. 11. High magnification scanning electron micrograph of the surface of an HDDR powder particle.



(a)

(b)

Fig. 12. Optical micrographs illustrating changes taking place during the HDDR process: (a) as-cast $\text{Nd}_{16}\text{Fe}_{76}\text{B}_8$ showing the typical plate-like grains of $\text{Nd}_2\text{Fe}_{14}\text{B}$ with the intercrystalline neodymium-rich material (dark regions); (b) $\text{Nd}_{16}\text{Fe}_{76}\text{B}_8$ after the HDDR process – the distribution of the neodymium-rich material is identical to that in (a) but the $\text{Nd}_2\text{Fe}_{14}\text{B}$ regions now consist of extremely fine grains of this phase.

however, that these areas consist of many fine grains of $\text{Nd}_2\text{Fe}_{14}\text{B}$. Transmission electron microscopy studies show the fine-grain structure more clearly (see Fig. 15) and also provide further evidence that the neodymium-rich material does not appear to be distributed between the very fine grains but remains distributed essentially as in the as-cast condition and as a result plays a part only in aiding the hot-pressing process. Subsequent annealing should redistribute the neodymium-rich material more uniformly; if this can be achieved without excessive grain growth, an improvement in the intrinsic coercivity should be observed. These experiments are under way in this laboratory.

Figure 16 shows the Kerr effect micrographs of HDDR powder which has been processed at temperatures slightly above the optimum necessary to produce the highest coercivity. Both figures exhibit very large (greater than $30\ \mu\text{m}$) grains which are a result of processing at too high a temperature.

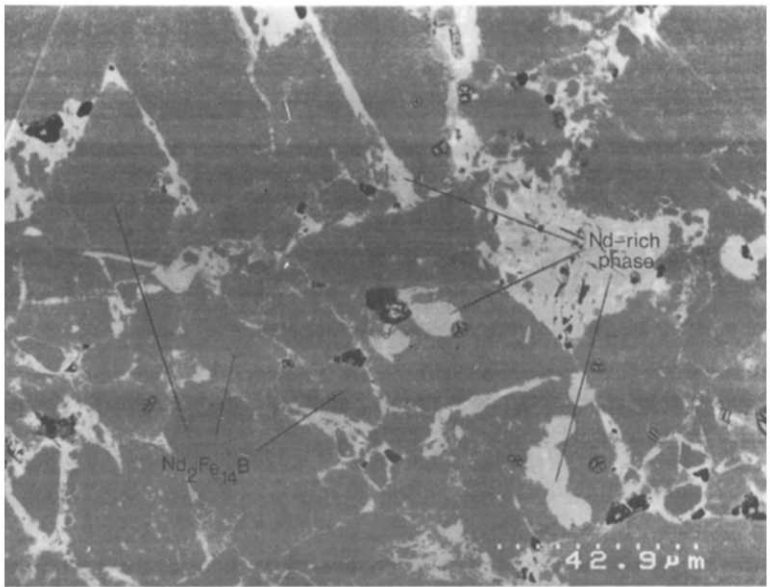


Fig. 13. Scanning electron micrograph of hot-pressed HDDR magnet. The dark regions are fine-grained $\text{Nd}_2\text{Fe}_{14}\text{B}$ and the light regions are neodymium-rich material.



Fig. 14. Fracture surface of hot-pressed HDDR magnet revealing uniform fine-grain size.

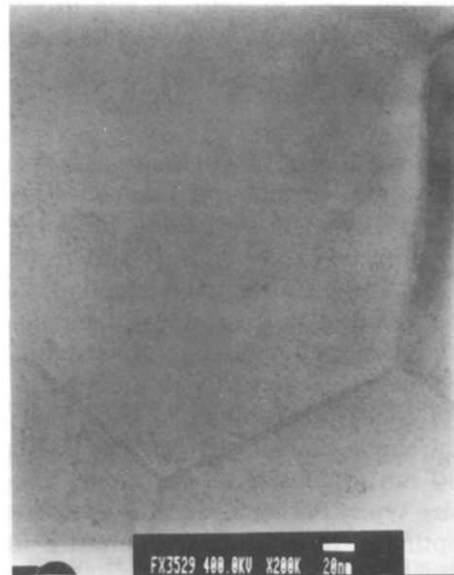


Fig. 15. Transmission electron micrograph of hot-pressed magnet showing no evidence of neodymium-rich material at grain boundaries.

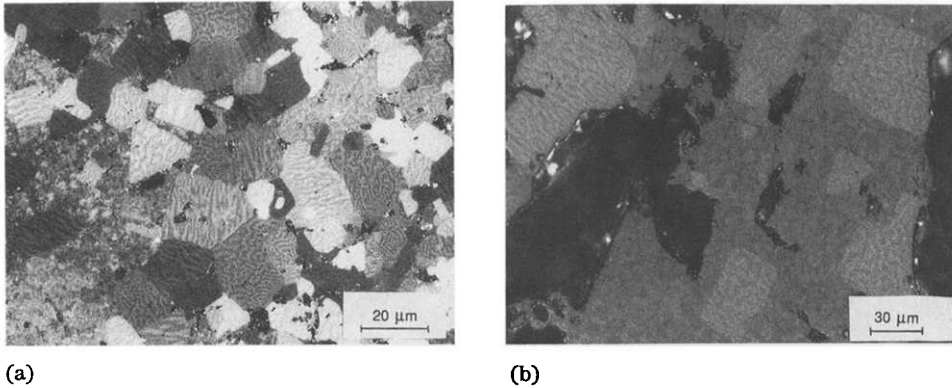


Fig. 16. (a) Random and (b) oriented grains in $\text{Nd}_{16}\text{Fe}_{76}\text{B}_8$ and $\text{Nd}_{16}\text{Fe}_{75.9}\text{B}_8\text{Zr}_{0.1}$ HDDR material viewed under polarized light to reveal magnetic domains.

The difference between the micrographs is that Fig. 16(a) shows the microstructure of the $\text{Nd}_{16}\text{Fe}_{76}\text{B}_8$ material where the grains have a very random orientation distribution, which is evident from their shape and domain structure, while Fig. 16(b) shows the microstructure of the $\text{Nd}_{16}\text{Fe}_{75.9}\text{B}_8\text{Zr}_{0.1}$ alloy where the large rectangular grains are growing with sides parallel to one another and with the same domain structure within each of the large grains, confirming that they have grown from oriented submicron grains characteristic of the highly anisotropic material, which produces magnets with a high remanence value.

8. Conclusions

(1) HDDR magnets are a new family of magnets different from both the conventional sintered magnets and the GM Magnequench products. High coercivity magnets can be produced without having to reduce the material to approximately 3 μm powders or the use of melt-spinning techniques.

(2) The processing involves the careful manipulation of the reactions between $\text{Nd}_2\text{Fe}_{14}\text{B}$ and hydrogen gas. By causing the alloy to disproportionate and then recombine into an ultrafine microcrystalline structure, a high degree of intrinsic coercivity is induced in the material. The optimum crystal size for these materials is of the order of about 300 nm, *i.e.* close to that of the single-domain size for $\text{Nd}_2\text{Fe}_{14}\text{B}$ and some way between the approximately 30 nm grain size of melt-spun ribbon and the approximately 10 μm grain size typical of sintered magnets. Under small-scale laboratory conditions the optimum processing temperature for $\text{Nd}_{16}\text{Fe}_{78}\text{B}_8$ material was found to be 755–785 °C.

(3) Isotropic hot-pressed magnets could be produced from $\text{Nd}_{16}\text{Fe}_{76}\text{B}_8$ material with remanences of about 695 mT, coercivities of around 1250 kA m^{-1} and densities of approximately 100%. The hot-pressing temperature

was found to be not very critical and good properties were obtained in the temperature range 730–760 °C.

(4) Isotropic hot-pressed magnets could be die upset to enhance the remanence with a slight reduction in the coercivity of the magnet. The results obtained indicate that a fully anisotropic magnet could be produced provided that a height reduction at the die-upsetting stage of around 80% could be achieved.

(5) Additions of 0.1 at.% Zr were found to produce highly oriented material without any great loss in coercivity. The degree of alignment in the powder was found to be about 95%. Increasing the amount of zirconium to 0.2 or 0.3 at.% resulted in poorer magnetic properties under the conditions of the experiment. The powder produced from $\text{Nd}_{16}\text{Fe}_{75.9}\text{Zr}_{0.1}\text{B}_8$ material was epoxy bonded into an anisotropic magnet with a $BH(\text{max})$ of 150 kJ m^{-3} .

(6) Microstructural investigations of $\text{Nd}_{16}\text{Fe}_{75.9}\text{Zr}_{0.1}\text{B}_8$ material subjected to the HDDR treatment revealed that the large rectangular grains tend to grow with a preferred orientation. This is in agreement with the observed high remanences obtained with this material.

Acknowledgments

We would like to thank CEAM, EURAM and SERC for research funds, REP (particularly G. Mycock) for helpful discussions and the provision of cast alloys, Dr. X. J. Zhang for useful discussions and Dr. K. G. Knoch for providing the transmission electron micrograph. Dr. M. L. H. Wise is thanked for the spark cutting and Dr. M. J. Wyborn and P. Bray of GEC for the provision of hot-pressing facilities and for their help with the experiments.

References

- 1 P. J. McGuinness, E. J. Devlin, I. R. Harris, E. Rozendaal and J. Ormerod, *J. Mater. Sci.*, **24** (1989) 2541.
- 2 T. Takeshita and R. Nakayama, *Proc. 10th Int. Workshop on Rare Earth Magnets and Their Applications, Kyoto, 1989*, p. 551.
- 3 P. J. McGuinness, X. J. Zhang, X. J. Yin and I. R. Harris, *J. Less-Common Met.*, **158** (1990) 359.
- 4 P. J. McGuinness, X. J. Zhang, H. Forsyth and I. R. Harris, *J. Less-Common Met.*, **162** (1990) 379.
- 5 A. S. Kim, to be published.
- 6 T. Takeshita and R. Nakayama, *Proc. 11th Int. Workshop on Rare Earth Magnets and Their Applications, Pittsburgh, PA, 1990* p. 7.
- 7 I. R. Harris and P. J. McGuinness, *Proc. 11th Int. Workshop on Rare Earth Magnets and Their Applications, Pittsburgh, PA, 1990*, p. 29.
- 8 I. R. Harris and P. J. McGuinness, *J. Less-Common Met.*, **172** (1991) 1273.
- 9 X. J. Zhang, P. J. McGuinness and I. R. Harris, *J. Appl. Phys.*, **68**(8) (1991) 5838.
- 10 P. J. McGuinness, X. J. Zhang, X. J. Yin, K. J. Knoch, M. J. Wyborne and I. R. Harris, *J. Magn. Magn. Mat.*, **104** (1992) 1169.
- 11 X. J. Zhang, P. J. McGuinness and I. R. Harris, to be published.
- 12 M. Tokunaga, Y. Nozawa, K. Iwasaki, S. Tanigawa and H. Harada, *J. Magn. Magn. Mater.*, **80** (1989) 80.